



Isoconversional and Model-fitting Approaches to Kinetic and Thermoanalytic Study of Lanthanum Oxalate: Nonlinear Relationship between Kinetic Parameters

Himansulal Nayak ^{a*}

^a Department of Chemistry, College of Basic Science and Humanities, Orissa University of Agriculture and Technology, Bhubaneswar- 751003, Odisha, India.

Author's contribution

The Author HN designed the study, performed the statistical analysis, wrote the protocol, and wrote the first draft of the manuscript, managed the analyses of the study and literature searches. The author read and approved the final manuscript

Article Information

DOI: 10.9734/AJOCS/2023/v13i2235

Open Peer Review History:

This journal follows the Advanced Open Peer Review policy. Identity of the Reviewers, Editor(s) and additional Reviewers, peer review comments, different versions of the manuscript, comments of the editors, etc are available here: <https://www.sdiarticle5.com/review-history/98539>

Original Research Article

Received: 05/02/2023

Accepted: 08/04/2023

Published: 21/04/2023

ABSTRACT

The data for the nonisothermal and isothermal thermal decompositions of lanthanum oxalate have been analysed using the model-free and model-fitting kinetic techniques. When applied to nonisothermal data using the Coat-Redfern(CR) equation, the widely used model-fitting approach that results excellent fitting for both isothermal and nonisothermal data but produces very ambiguous values of the Arrhenius parameters. These values cannot be compared to those obtained from isothermal experiments. On the other hand, the model-free strategy represented by the iso-conversional method, such as Flynn-Wall-Ozawa (FWO) and Kissinger-Akahira-Sunose

*Corresponding author: E-mail: himansu110@gmail.com;

(KAS), emphasize proportionate variation of the activation energy with the degree of conversion for both isothermal and nonisothermal experiments. The model free approach is recommended as a reliable way for obtaining consistent kinetic information from both isothermal and non-isothermal data. Despite their linear correlation, the kinetic parameters do not exhibit isokinetic behaviour. Thus, utilising Nonlinear Compensation Law, a greater association between kinetic triplets was examined.

Keywords: *Nonisothermal decomposition; model free and model fitting methods; kinetic parameters; thermodynamic parameters; isokinetic behaviour; nonlinear compensation law.*

1. INTRODUCTION

For many researchers, kinetic study of thermal breakdown processes has been a particularly interesting topic. The breakdown processes and kinetics go hand in hand. Understanding the mechanism enables the postulation of kinetic equations, or the other way around [1]. It is obvious that choosing the right model is a crucial step in kinetic analysis. Several scholars have assessed how a model may support experimental data [2–3]. The kinetics of non-isothermal processes can be investigated using a variety of techniques. They include iso-conversional model-free techniques, statistical techniques, and the Coats-Redfern (CR) method. For the defined conversion intervals, activation energy, or E_a values, were obtained [4] by utilising the iso-conversional model-free procedures such as modified Kissinger-Akahira-Sunose (KAS) and the Kissinger method, respectively. E and the change in entropy ΔS^* for the creation of the activated complex from the reagents have also been shown to be linearly related. These dependencies are connected to the presumption that the composites under study experienced the same kinetic mechanisms of heat deterioration [5].

The Coat-Redfern (CR) method exhibits nonlinear trends for reactions with heterogeneous mechanisms, and the reaction models and kinetic parameters cannot be retrieved from the curves. As a result, the method is often inappropriate for determining kinetic parameters [6]. The average findings of non-isothermal trials may be compared with isothermal analysis since using the standard methods in non-isothermal kinetics leads in highly ambiguous Arrhenius parameter values that cannot be properly compared with isothermal values [7]. The iso-conversional method serves as the foundation for an alternative model-free methodology. The application of this model-free method in both isothermal and non-isothermal kinetics helps in

avoiding issues that result from the inappropriate evaluation of reaction model. The model-free methodology allows the proportionate variation of activation energy with the degree of conversion. As a result, it is possible to estimate reaction rates with accuracy and make mechanistic conclusions [8]. The exact activation energy cannot therefore be inferred from a single non-isothermal curve. On the other hand, the correct kinetic parameters can be identified clearly when a collection of curves is recorded using various heating regimens [9]. According to experimental findings, the values of the kinetic parameters obtained using the model-free and model-fit approaches are in close agreement and can be utilised to comprehend the decomposition mechanism of solid-state reactions [10].

The present work apply both model-fitting integral and model-free isoconversional methods to have significant and appreciable picture about the decomposition mechanism of Lanthanum Oxalate Decahydrate. The degree of reliability of parameters obtained from both the techniques are also studied. The kinetic parameters which generally fit to linear kinetic compensation law [11] have been revisited for better correlation from their nonlinearity and the authenticity of the kinetic data was tested by fitting into nonlinear compensation law so as to obtain true values.

2. MATERIALS AND METHODS

Lanthanum Oxalate Decahydrate, was prepared as per our earlier work [12], using high purity AR grade $\text{La}(\text{NO}_3)_3$ and Ammonium Oxalate purchased from Sigma –Aldrich. Ammonium Oxalate solution was added drop wise to the $\text{La}(\text{NO}_3)_3$ solution with stirring for 30 min. White precipitate of Lanthanum Oxalate decahydrate (LaOx) obtained was washed with distilled water and absolute alcohol. For one hour, the precipitate was allowed to stand at room temperature. Powdered lanthanum oxalate decahydrate was produced after being ground in an agate mortar and dried in a vacuum oven at

70°C. By using FTIR, TEM, XRD, etc., the obtained Lanthanum oxalate powder was characterised. The calcination products were produced by heating for 1 hour at a range of temperatures (200-800°C) in a static air atmosphere. The results of the thermal analysis were used to determine the calcination temperatures. LaOx-200 designates the calcination product at 200°C, and the calcination products are indicated throughout the article by the oxalate designation and the temperature used. Thermal TG/ DTA analysis of lanthanum oxalate were carried out at the heating rates of 3, 5 and 7°C min⁻¹ up to 900°C in a dynamic atmosphere of air (20 ml/min), using SHEMATZU DTG 50 analyzer. The same sample was also subjected to isothermal breakdown at temperatures of 643, 653, and 663K.

3. RESULTS AND DISCUSSION

3.1 FTIR Analysis

The FT-IR 410 JASCO(JAPAN) on KBr support was used to obtain the IR spectra across the wavelength range of 4000-100 cm⁻¹. La₂(C₂O₄)₃·10H₂O and the Lanthanum oxalate calcined at 200°C (Fig. 1) are quite similar in structure, with the oxalate anions' (1750-640 cm⁻¹) and the water of hydration (3440,1640 cm⁻¹) absorption bands being the most similar. IR-spectrum of Lanthanum oxalate calcined at 300°C, the C₂O₄²⁻ species are weaker than CO₃²⁻ and exhibit distinctive CO₃²⁻ like bands at 2350 cm⁻¹ and 1800-400 cm⁻¹. Further heating at 400°C causes lose water of bands due to hydration absorption. The fundamental modes of

vibration of the CO₃²⁻ species are weakened and distinct band structure appear at 1600 -1300cm⁻¹ corresponding to characteristic absorptions of oxycarbonates. The IR-spectrum LaOx-550 exhibits substantial oxycarbonate with additional bands at 1060-870 cm⁻¹. The La-O vibrational bands appear at 730-500 cm⁻¹. The IR-spectrum of lanthanum Oxalate calcined at 800°C, shows no absorptions due to oxycarbonate species. Lattice vibration modes of La₂O₃ are related to the absorptions below 700 cm⁻¹. Given that La₂O₃ is a recognised basic oxide, the weak bands at 1600, 1500, and 1380 cm⁻¹ are most likely caused by carbonate and moisture on the surface.

3.2 TEM Analysis

The general morphologies and microstructure of the sample was investigated by transmission electron microscopy(TEM, JEM-100CX II, Japan Electronics Co., Ltd., Japan), which illustrates that many needle-shaped particles are in the size range of 100 nm. The TEM images (Fig. 2) reveal that most of the particles are uniform in size.

3.3 Thermal Analysis with X-ray Diffraction

Using a rising temperature approach at 10 min⁻¹ till 900°C in air, the non-isothermal decomposition of the uniform 300 mesh lanthanum oxalate decahydrate La₂(C₂O₄)₃·10H₂O is examined (Fig. 4). Shimadzu XRD-6000 diffractometer X-ray diffraction patterns were obtained by scanning

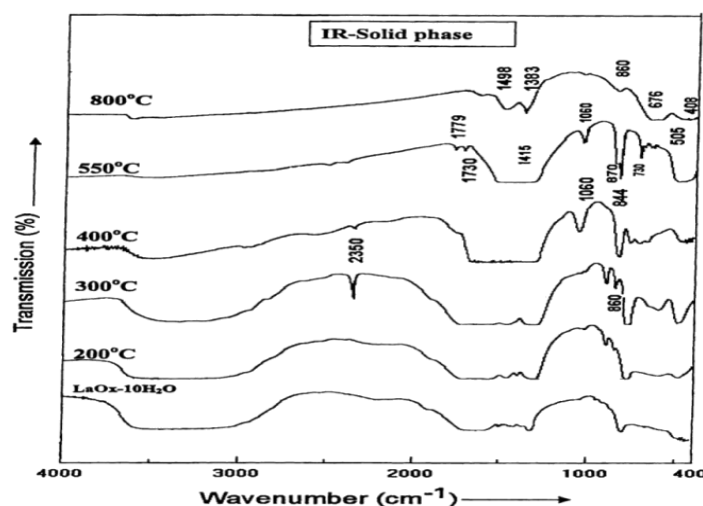


Fig. 1. FTIR curves of Lanthanum Oxalate at room temperature at temperatures 200, 300,400,550 & 800°C

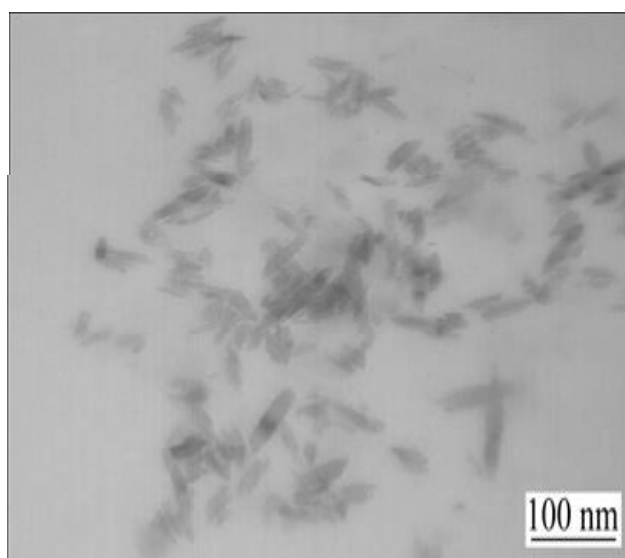


Fig. 2. TEM image of lanthanum Oxalate decahydrate

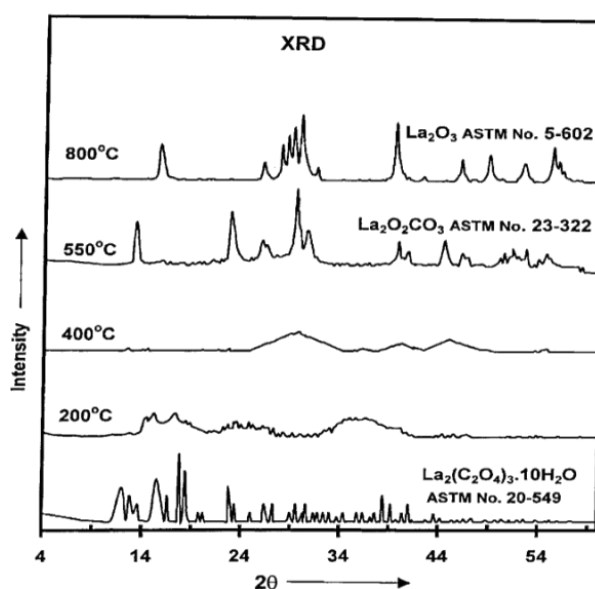


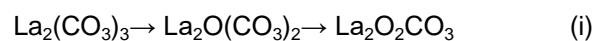
Fig. 3. X-Ray diffraction patterns of decomposition products of lanthanum oxalate obtained at different temperatures

the angular range $100 \leq 2\theta \leq 900$ using $\text{CuK}\alpha$ radiation ($\lambda = 1.5418 \text{ \AA}$). Intermediates and final solid products were characterised by FTIR-spectroscopy and X-ray diffraction (XRD). The results show that $\text{La}_2(\text{C}_2\text{O}_4)_3 \cdot 10\text{H}_2\text{O}$ dehydrates decomposed in stepwise at $90\text{--}360^\circ\text{C}$. The intermediates, $\text{La}_2(\text{C}_2\text{O}_4)_3$, $\text{La}_2\text{O}(\text{CO}_3)_2$ and $\text{La}_2\text{O}_2\text{CO}_3$, were formed at 400 , 425 and 470°C , respectively. The final product La_2O_3 obtained at 800°C [12].

The XRD patterns (Fig. 3) of LaOx-200 and LaOx-400 indicates that the products are

amorphous indicating $\text{La}_2(\text{CO}_3)_3$ product to be amorphous.

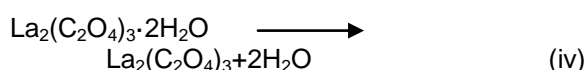
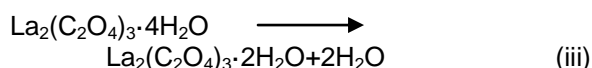
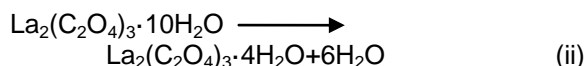
The conversion of $\text{La}_2(\text{CO}_3)_3$ to $\text{La}_2\text{O}(\text{CO}_3)_2$ which converts immediately to $\text{La}_2\text{O}_2\text{CO}_3$ as follows [13]:



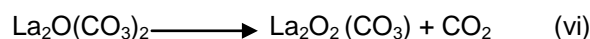
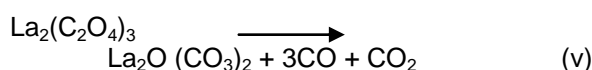
Events IX, X, and XI took place between $420\text{--}550^\circ\text{C}$. The aforesaid reaction is supported by the IR spectra (Fig. 1) and XRD patterns (Fig. 3). The comparable X-ray pattern for LaOx-550

displays the crystalline $\text{La}_2\text{O}_2\text{CO}_3$ pattern. X-ray pattern of LaOx-800 reveals a crystalline phase of La_2O_3 in support of FTIR.

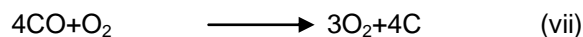
Loss of water took place in three stages as follows [Table 1]



The fourth stage begins at 375°C involving decomposition of $\text{La}_2(\text{C}_2\text{O}_4)_3$ to $\text{La}_2\text{O}_2(\text{CO}_3)$, a dioxy monocarbonate [13].



Although the decomposition of oxalate is endothermic, the exotherms appear in DTA is due to secondary reaction of CO and O_2 (Fig. 4).



3.4 Kinetic Analysis

For determination of Kinetic parameters, the TG curves are obtained at heating rates of 3, 5, and 7°C min^{-1} (Fig. 5), show that the sample degraded between 370°C and 550°C . The maximum decomposition temperature, T_m and inception temperature T_0 increase with rate of heating. Furthermore, the area under the decomposition peak increased with increasing heating rate (Fig. 6).

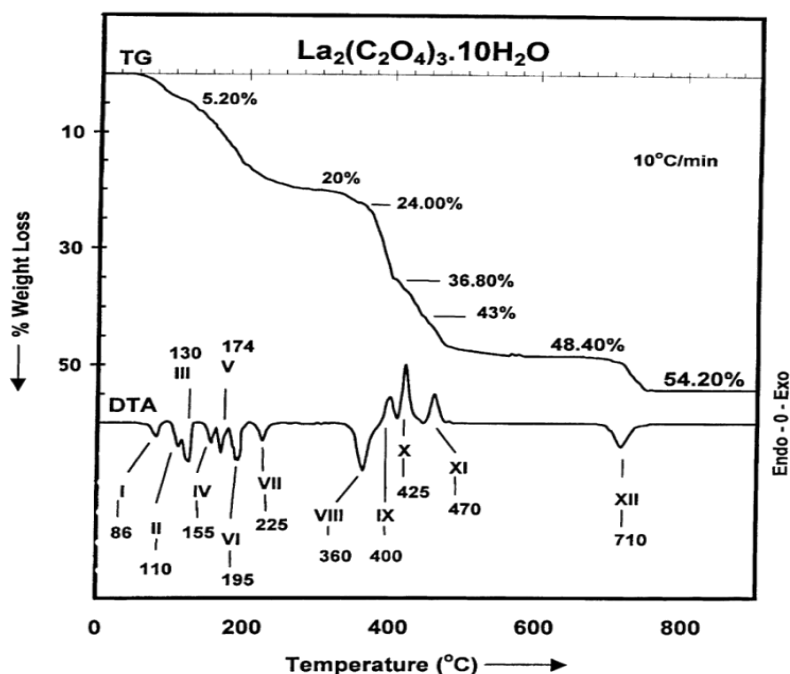


Fig. 4. TG-DTA curve of Decomposition of Lanthanum Oxalate decahydrate heated upto 900°C

Table 1. Step wise Degradation data of $\text{La}_2(\text{C}_2\text{O}_4)_3 \cdot 10\text{H}_2\text{O}$

Temperature Range/ $^\circ\text{C}$	Mass change (%)		Solid residue
	Theoretical	Experimental	
30-225	14.7	14.5	Hexahydrate
225-300	5.2	4.98	Dihydrate
300-375	4.98	5.12	Anhydrous oxalate
375-600	23.7	28.52	$\text{La}_2\text{O}_2\text{CO}_3$
600-750	6.19	6.92	La_2O_3

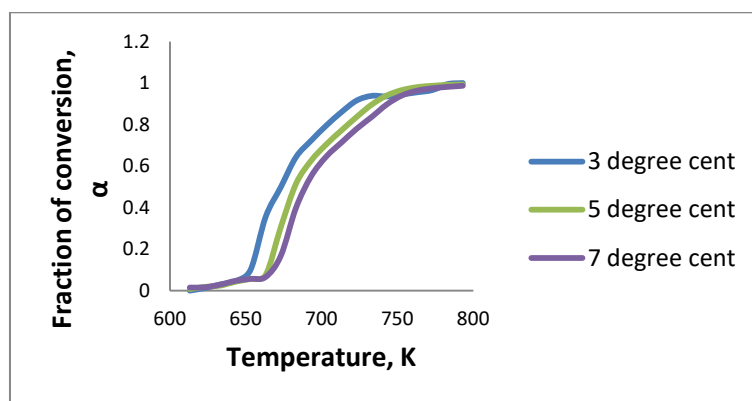


Fig. 5. Thermogravimetric curves for decomposition of lanthanum oxalate at different rate of heating

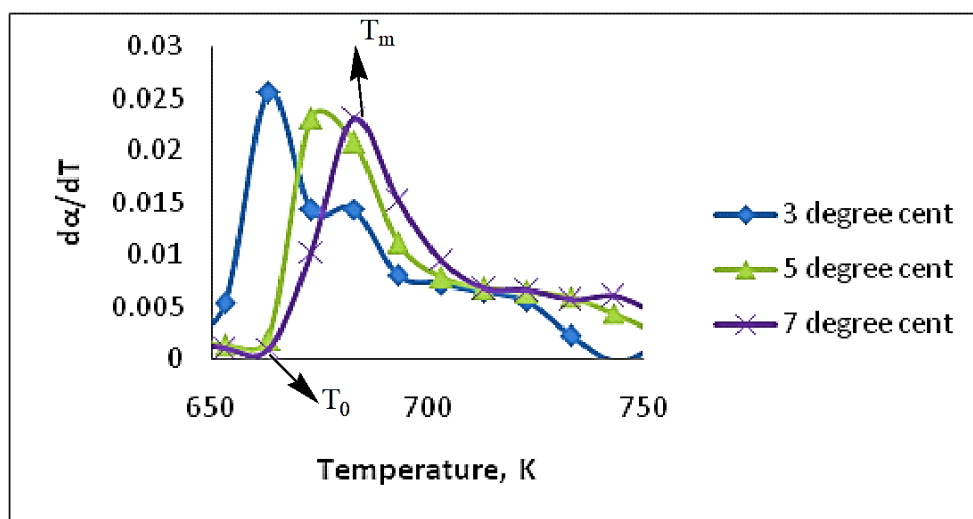


Fig. 6. Derivative curves of lanthanum oxalate decomposition at different rates of heating

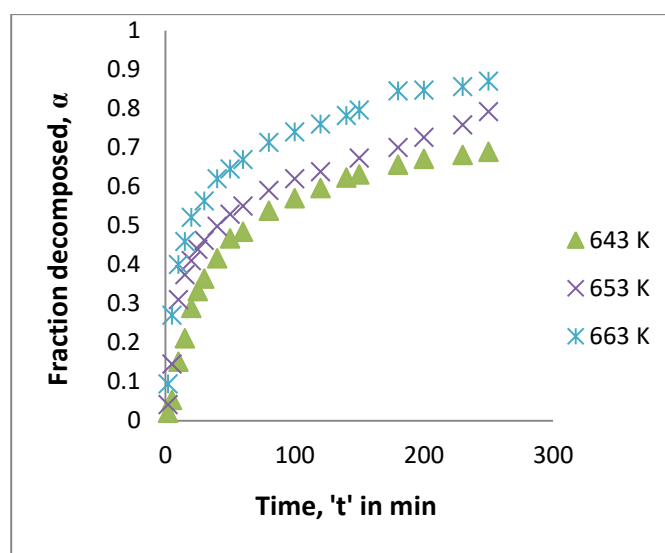


Fig. 7. Conversion- time curve for isothermal decomposition of lanthanum oxalate

Isothermal decomposition curves for the lanthanum oxalate at three different temperatures also exhibit similar behaviour as in case of non-isothermal study and the “conversion-time” curve i.e. ‘ α -t’, plot show upward shift with time, at higher temperatures (Fig. 7).

3.4.1 Nonisothermal method

Model-fitting Coat Redfern (CR) and iso-conversional model free (FWO & KAS) approaches were both used to determine kinetic parameters [14,15]. At the temperature range of 380-480⁰C, or 653-753K (steps VIII-XI), for the best-fitting F3 mechanism model functions, $g(\alpha)$, and correlated by the compensation law[16], the Arrhenius parameters E and log A are derived. Using the CR equation, the slopes and intercepts of the graphs $1/T$ vs. $\log [g(\alpha)/T^2]$ at three different heating rates are obtained (Fig. 8).

$$\log [g(\alpha)/T^2] = \log [AR/\beta E] - E/2.303RT \quad (3)$$

Iso-conversional analyses allow a complex processes to be detected by variation of E_α with α . The Kissinger–Akahira–Sunose(KAS) method is used in the form

$$\ln(\beta/T_\alpha^2) = \ln (A_\alpha R)/(E_{\alpha}g(\alpha)) - E_\alpha/R T_\alpha \quad (4)$$

Thus, for different values of α , $\ln (\beta/T_\alpha^2)$ and $1/T_\alpha$, were obtained from thermal curves at different heating rates, and straight lines are obtained for each ‘ α ’ (Fig. 9). The apparent activation energies, E and pre-exponential factors, logA are evaluated from the slopes and intercepts respectively for each ‘ α ’.

Similarly the Flynn–Wall–Ozawa (FWO) method is used in the form [17].

$$\ln \beta = \ln (A_\alpha E_\alpha) / (Rg(\alpha)) - 5.331 - 1.052 E_\alpha / (RT_\alpha) \quad (5)$$

A graph between $\ln \beta$ and $1/T_\alpha$, are plotted for different α 's (Fig. 10) which allow us to evaluate the E and logA for different α 's The average values are calculated for comparison (Table 3).

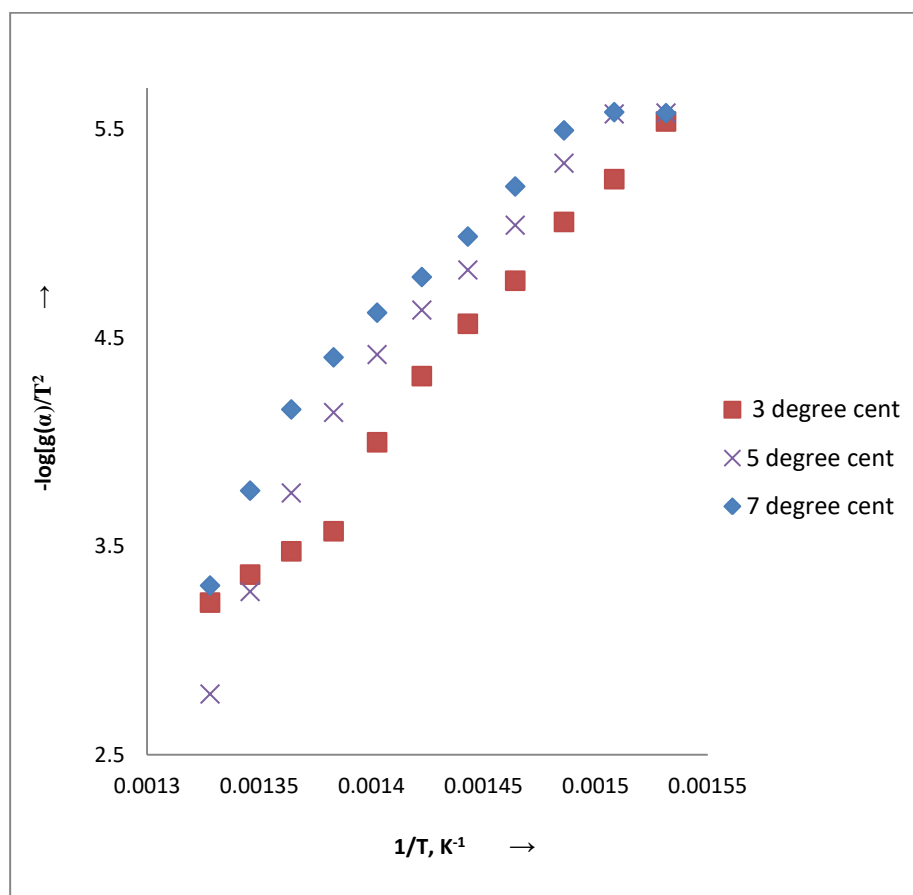


Fig. 8. Variation of $-\log[g(\alpha)/T^2]$ with $1/T$ at different rate of heating

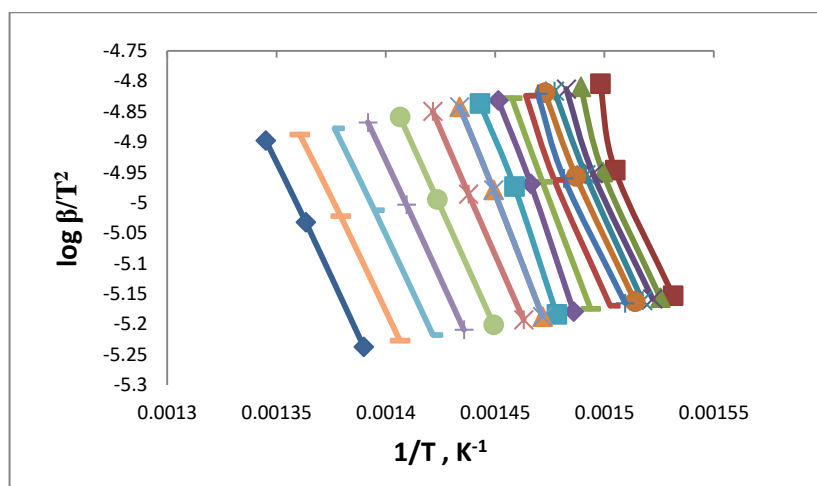


Fig. 9. $\ln(\beta/T^2_\alpha)$ vs $1/T_\alpha$ plots

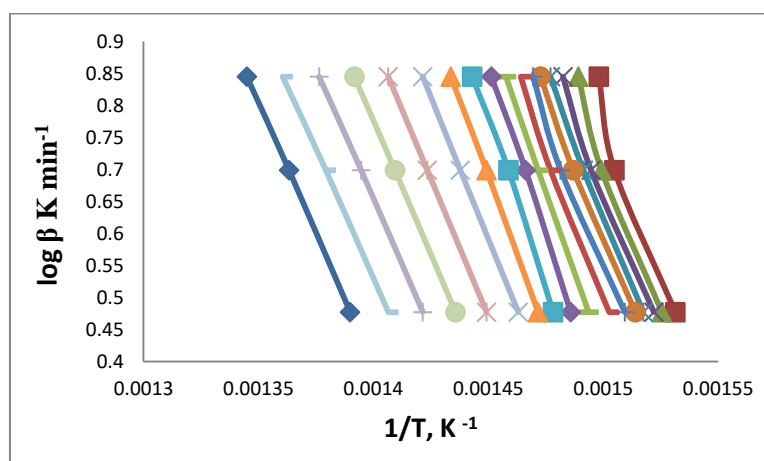


Fig. 10. $\log \beta - 1/T$ plots for E of the first endothermic peak by FWO method

3.4.2 Isothermal method

Isothermal study in the temperature region 643-663K allow the calculation of kinetic parameters by correlating mechanism model function, $g(\alpha)$ with time, t (Fig. 11). The plot is a straight line with rate constant, k calculated from the slope using the equation:

$$g(\alpha) = kt + c \quad (1)$$

The rate, k was obtained at three different isothermal temperatures and presented [Table 3]. The kinetic parameters E and A are obtained from slope and intercepts respectively, from the plot of $\ln k$ vs $1/T$ (Fig. 12) using the Arrhenius equation;

$$\ln k = \ln A - E/RT \quad (2)$$

The isothermal and non-isothermal kinetic parameters are compared and presented in Table 2.

The apparent activation energy for the degradation of lanthanum Oxalate is not same at all conversion, α (Fig. 13), indicates the existence of a complex multistep mechanism that occurs in the solid state. The kinetic and thermodynamic parameters for both model fitting and model free methods are presented [Table 2].

The values of apparent activation energy (E_a) calculated by model free (KAS and FWO) methods are in conformity with the reported activation energy in many studies i.e. 177.5 kJ/mol [18] and lower than values of E_a calculated by integral non-isothermal (Coat-Redfern) and isothermal methods.

Thermodynamic parameters e.g. entropy of activation (ΔS^*), enthalpy of activation (ΔH^*) and Gibbs free energy (ΔG^*) were calculated using Equations (6)-(9).

$$A = (kT/h)e^{(\Delta S^*/R)} \quad (6)$$

$$\Delta H^* = \Delta E - RT \quad (7)$$

$$\Delta G^* = \Delta H^* - T\Delta S^* \quad (8)$$

where h and k are Planck's constant and Boltzmann constant respectively.

With an increase in activation energy, it has been found that the entropy of activation also

increases. The fact that the value of ΔG is positive indicates that the Lanthanum oxalate decomposition process is not spontaneous. It is noted that the activation energy is nearly equal to the activation enthalpy, which suggests that lanthanum oxalate is in the condensed phase between 653 and 753 K. When ΔS^* values for iso-conversional procedures are negative, it means that the activated complex for that method has a higher degree of arrangement (lower entropy) than it had in the initial state. Table 3 presents information on kinetic and thermodynamic characteristics gathered by various techniques.

Table 2. Kinetic and Thermodynamic parameters of $\text{La}_2(\text{C}_2\text{O}_4)_3$ decomposition, by various methods

Methods used	β , ($^{\circ}\text{Cmin}^{-1}$)	E , (kJmol^{-1})	$\log A$, (min^{-1})	ΔH^* , (kJmol^{-1})	ΔS^* ($\text{Jmol}^{-1}\text{K}^{-1}$)	ΔG^* (kJmol^{-1})
Coat-Redfern	3	230.33	16.00	224.76	46.34	193.71
	5	255.50	17.94	249.92	83.46	194.01
	7	209.26	14.32	203.69	14.26	194.13
	Average	231.70	16.09	226.12	48.02	193.95
Isoconversional	FWO	167.98	11.05	162.41	-48.46	194.88
	KAS	165.26	10.06	159.69	-52.25	194.70
Isothermal		303.03	23.16	298.77	148.19	199.48

Table 3. Rate constants obtained at different isothermal temperatures

k , sec^{-1}	T , K	$1/T$, K^{-1}	$-\log k$
0.038819	643	0.00155521	1.41096
0.069832	653	0.001531394	1.15595
0.215161	663	0.001508296	0.66724

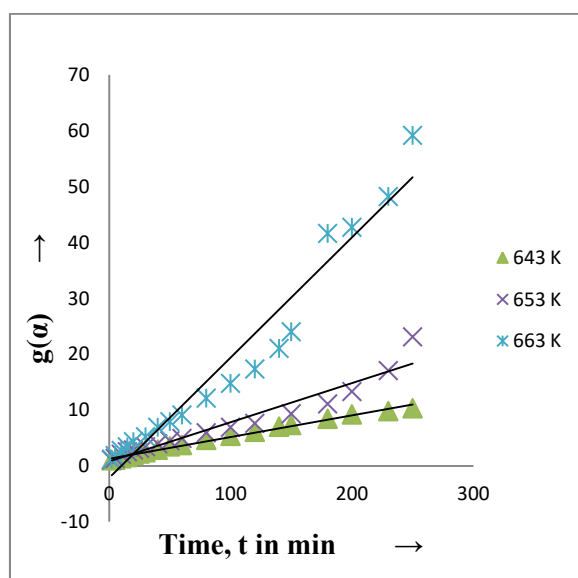


Fig. 11. Variation of $g(\alpha)$ with time, t at different temperatures

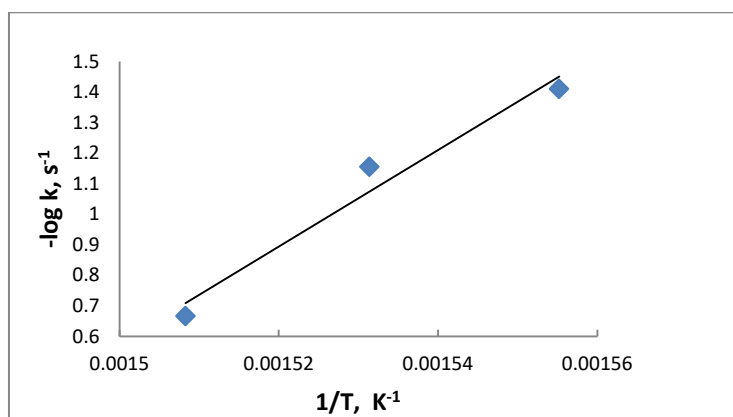


Fig. 12. Variation of T^{-1} with $-\log k$ during isothermal decomposition of lanthanum oxalate

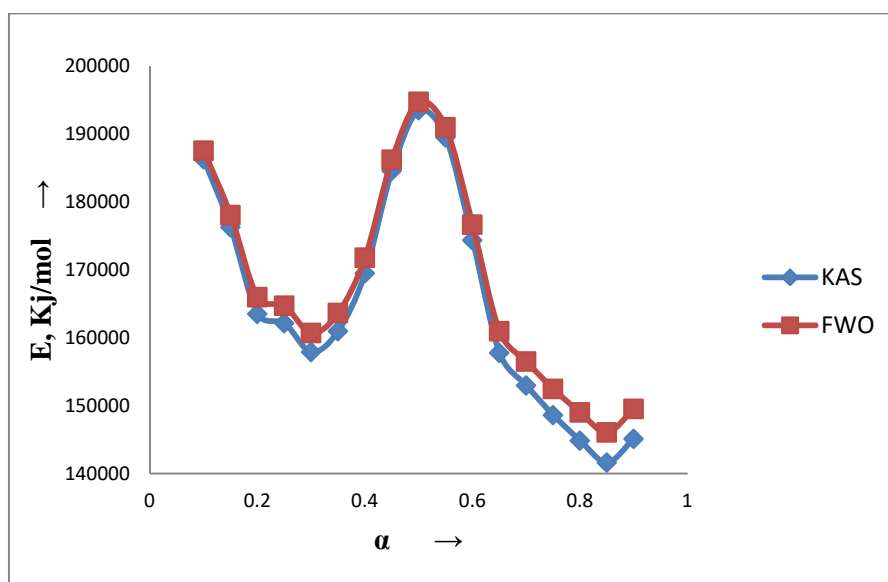


Fig. 13. Variation of activation energies, E with degree of conversion, α

In case of isothermal method the E has the highest value and this discrepancy may be due to the F3 mechanism which could be different in case of isothermal study. Moreover the rising temperature technique that uses CR equation with F3 model function also reported higher value of E. This may be attributed to the fact that, for $\alpha < 0.70$ in the chosen temperature range and the plot of $\log[g(\alpha)/T^2]$ versus $1/T$ is linear, indicating that the reaction is a single mechanism. However for extents of reaction $\alpha > 0.7$ the reaction has multi model mechanisms, for which the CR eqn. cannot be used showing a nonlinear trend (Fig. 8). Therefore it is ascertained that kinetics of complex reactions, where the reaction model changes with the extent of reaction, cannot be analysed with CR method with absolute correctness.

Further from isoconversional methods it is evident that E depends on α , demonstrating that the decomposition reaction process of the lanthanum oxalate is of complex kinetic mechanism [19]. Hence the kinetic parameters derived may be considered to be apparent and not true. The activation energies, E calculated by various methods are presented in bar diagram (Fig. 14).

3.4.3 Kinetic compensation effect

The change in apparent activation energy, E, is found to be followed by a change in $\ln A$. This phenomenon is known as the kinetic compensation effect (KCE), and it frequently coexists with the isokinetic point ($1/T_{iso}, \ln k_{iso}$). According to the Cremer-Constable relation, the

variations in pre-factor and apparent activation enthalpy exhibit a linear dependency [20].

$$\ln A = aE + b \quad (9)$$

Where a and b are constant coefficients for a series of related rate process and are called compensation parameters. The rate constant, 'k' is temperature dependent, and is usually described well by Arrhenius relationship:

$$k = A e^{-E_a/RT} \quad (10)$$

$$\ln A = \ln k + E/RT \quad (11)$$

Although the experimental data showed that a plot of $\ln A$ vs E (Fig. 16) and $\log k$ vs $1/T$ (Fig. 15) different methods in the temperature range 653K-753K, are all linear, but fail to display a single point of concurrence i.e. isokinetic point ($1/T_{iso}$, $\log k_{iso}$). Hence the kinetic parameters exhibit a false compensation effect and are with their apparent values.

3.4.4 Non linear Compensation law and kinetic parameters

The correlation derived between the kinetic parameter E and $\log A'$ from TG curves can be described by means of Non linear compensation law [21] expressed as

$$\log A' = (RT_{0.1} \ln 10)^{-1} E + \log(\beta E/T_{0.1}^2) - 1.85 \quad (12)$$

Where $T_{0.1}$ is the temperature at which the conversion attains a degree of 0.1 ($\alpha = 0.1$). The equation is not a linear and therefore it is not an iso-kinetic relation. However the relationship becomes iso-kinetic provided $\log(\beta E/T_{0.1}^2)$ is constant, which is not found in the present work. The true values of pre factor $\log A'$ is varies with rates of heating, β and presented along with $\log(\beta E/T_{0.1}^2)$ [Table 4] for both model fitting and model free methods of analyses.

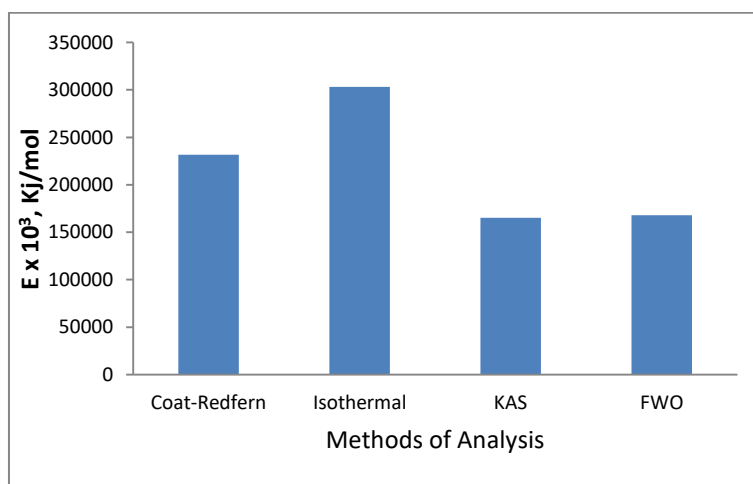


Fig. 14. Variation of activation energies with methods of analysis

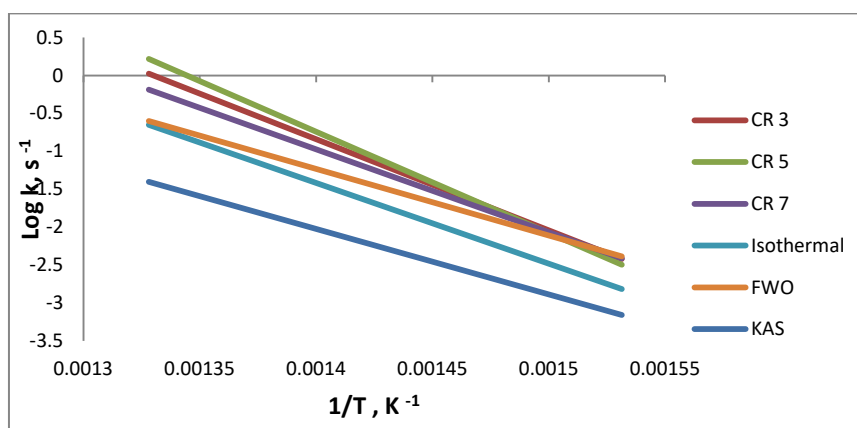


Fig. 15. Variation of log k with 1/T for different methods of analyses

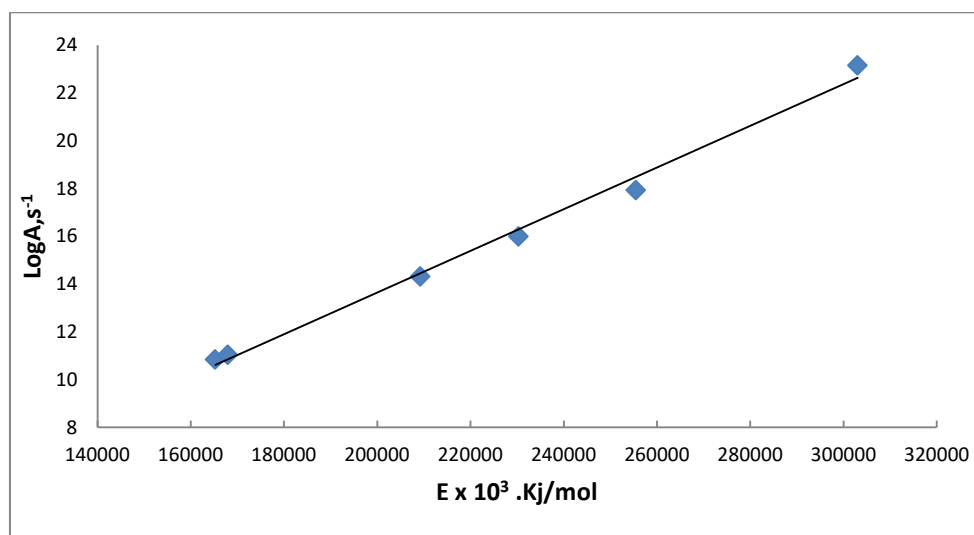


Fig. 16. Variation of log A with E and verification of Kinetic Compensation Effect

Table 4. Corrected approximation for pre-exponential factors using nonlinear compensation law

	β	$\log(\beta E/T_{0.1}^2)$	$\log A', (s^{-1})$
CR	3	0.2096	16.572
	5	0.4614	18.692
	7	0.5169	15.04
FWO	3	0.0725	11.657
	5	0.2792	11.632
	7	0.4214	11.715
KAS	3	0.0655	11.433
	5	0.2721	11.411
	7	0.4144	11.495

5. CONCLUSION

It was ascertained that using model-fitting techniques of kinetic analysis to data obtained under non-isothermal experimental settings does not allow for the accurate determination of the activation energy. As the ICTAC Kinetics Committee has advised [21], it is therefore required to employ a set of curves obtained under various heating regimens. As only one-step processes may be analysed using this methodology, it is also important to consider the nature of the reaction under study into account. Isoconversional techniques or the deconvolution of the separate steps, such as KAS and FWO, are required for more complicated or multi-step reactions. The kinetic parameters of the conversion of lanthanum oxalate to the equivalent carbonate follow kinetic compensation behaviour, but the result is an false compensation effect. Non-linear compensation rule, which is a good approximation, provides a

more accurate explanation of the relationship between E and logA.

COMPETING INTERESTS

There is not any potential conflicts of interest like employment, consultancies, honoraria, paid expert testimony, patent applications/registrations, and grants or other funding etc. There is no financial and personal relationships with other people or organizations that could inappropriately influence (bias) the work.

REFERENCES

1. Jach J. In "reactivity of solids" (Ed. J.H. De. Boer) Elsevier, Amsterdam. 1961; 334.
2. Jach J. The thermal decomposition of NaBrO₃ part I-Unirradiated material. J. Phys, Chem Solids. 1963;24: 63.

3. Galway AK. In "Int. Rev. Sc."Inorg. chem. Series II. Butterworth, London. 1975;10:147.
4. Boldyrev VV. Topochemistry of thermal decomposition of solids. *Thermochim. Acta.* 1986;100: 315.
5. Physiak J, Wasia BP. *J. Therm. Anal.* 1984;29:829.
6. Ebrahimi-Kahrizsangi R, Abbasi MH. Evaluation of reliability of coats-redfern method for kinetic analysis of non-isothermal TGA. *Trans. Nonferrous Met. Soc. China.* 2008;18:217-221.
7. Xia Yongjiang, XueHuaqing, Wang Hongyan, Li Zhiping, Fang Chaohe. Kinetics of isothermal and non-isothermal pyrolysis of oil shale. *Oil Shale.* 2011;28:415–424.
8. Sergey Vyazovkin and Charles A. Wight; Isothermal and non-isothermal kinetics of thermally stimulated reactions of solids. *Int. Rev. in Phy. Chem.* 1998;17:407- 433.
9. Pedro E. Sánchez-Jiménez, Luis A. Pérez-Maqueda, Antonio Perejón and José M. Criado.. Clarifications regarding the use of model-fitting methods of kinetic analysis for determining the activation energy from a single non-isothermal curve; *Chem. Cent. Journal.* 2013;7:25(Short Communication)
10. Słopiecka K, Bartocci P, Fantozzi F. Thermogravimetric analysis and Kinetic study of poplar wood pyrolysis. *Third International Conference on Applied Energy.* 2011;1687-1698.
11. Adonyi Z, Korosi G. Experimental study of non-isothermal kinetic equations and compensation effect. *Thermochim. Acta.* 1983;60:23-45.
12. Basma AA. Balboul AM. El-Roudi, Ebthal Samir AG Othman. Non-isothermal studies of the decomposition course of lanthanum oxalate decahydrate, *Thermochim. Acta.* 2002;387:109–114.
13. Nayak H, Pati SK, Bhatta D. Decomposition of γ -irradiated $\text{La}_2(\text{C}_2\text{O}_4)_3 + \text{CuO}$ mixture: A non-isothermal study. *Rad. Eff. and Def. in Solids.* 2004;159:93–106.
14. Simon P. Isoconversional methods-fundamental, meaning and application. *J. Therm. Anal. Calorim.* 2004;76:123.
15. Vyazovkin S, Wight CA. Model free and model fitting approaches to Kinetic analysis of isothermal and nonisothermal data. *Thermochim. Acta.* 1999;340/341:53.
16. Jankovic B. Kinetic analysis of the nonisothermal decomposition of potassium etabisulfite using the model-fitting and isoconversional (model-free) methods. *Chem. Eng. Journal.* 2008; 139:128–135.
17. Zhan Guang YU, Jun-xia Xu, Zhi-gao, Zhou Fang, Chiru-an. Kinetics of thermal decomposition of lanthanum oxalate hydrate ;*Trans. Nonferrous Met. Soc. China,* 2012,22: 925–934
18. Obaid AY, Alyoubi AO, Samarkandy AA, Al-Thabaiti SA, Al-Juaid SS, Ei-Bellihi AA, Ei-Deifallah HM. Kinetics of thermal decomposition of copper(II) acetate monohydrate. *J. Therm Anal Calorim.* 2000;61(3):985–994.
19. Bond GC, Keane MA, Kral H, Lercher JA. *Catal. Rev.-Sci. Eng.* 2000;42(3):319-327.
20. Zsako J. Kinetic analysis of thermogravimetric data xxxi. derivation of non-linear kinetic compensation law. *J. Therm. Anal.* 1998;54:921-929.
21. Vyazovkin S, Burnham AK, Criado JM, Perez-Maqueda LA, Popescu C, Sbirrazzuoli N. ICTAC Kinetics Committee recommendations for performing kinetic computations on thermal analysis data. *Thermochim. Acta.* 2011;520:1–19.

© 2023 Nayak; This is an Open Access article distributed under the terms of the Creative Commons Attribution License (<http://creativecommons.org/licenses/by/4.0>), which permits unrestricted use, distribution, and reproduction in any medium, provided the original work is properly cited.

Peer-review history:

The peer review history for this paper can be accessed here:

<https://www.sdiarticle5.com/review-history/98539>